Originally published in *Proceedings of the Fifth International Workshop on Compressible Turbulent Mixing*, ed. R. Young, J. Glimm & B. Boston.
ISBN 9810229100, World Scientific (1996).

Rayleigh–Taylor Instability Effects in Acceleration of Plane Solid Layer*

V. A. Rayevsky

All Russia Scientific Research Institute
of Experimental Physics
Nizhny Novgorod Region, RUSSIA

1 Introduction

During recent years, many laboratories in the world have been conducting research to develop devices that would accelerate solid bodies to hypersonic velocities above 10 km/s.

Applications of this research may involve, for example, the use of hypervelocity species to investigate spacecraft response to meteorite effects and to explore safety means. Plane liners are to be used to investigate equations of state for materials under high pressures.

The highest values achievable are those using plane liners because these are what allow the maximum use of the explosion energy of highly heated gas to drive the liner. Currently, the plane liner velocity achieved is about 13 km/s.

The further acceleration of the liner by increasing driver energy may appear less effective due to Rayleigh-Taylor instability which may result in the liner deformation and disruption, when the acceleration time is long and value high.

The perturbation growth during acceleration can be restrained by using liner materials as strong as possible having the least difference in density and thickness and also by optimizing the liner loading rate. This allows complete suppression of short-wavelength perturbations, i.e. having wavelength less than the liner thickness. However, a real layer would generally have certain differences in thickness and density, with the driver pressure being non-uniformly distributed over its surface. Therefore, given sufficient acceleration time, the layer is sure to be disrupted. It is of great interest to estimate the maximum velocity the plane liner can achieve, assuming RT instability as the sole restrictive consideration.

RT instability in solids has been studied since 1960. Even for small perturbations and the simplest elasto-plastic approximation, the instability in solids is much more

*This research was sponsored by the International Scientific Foundation, Grant NM4000.

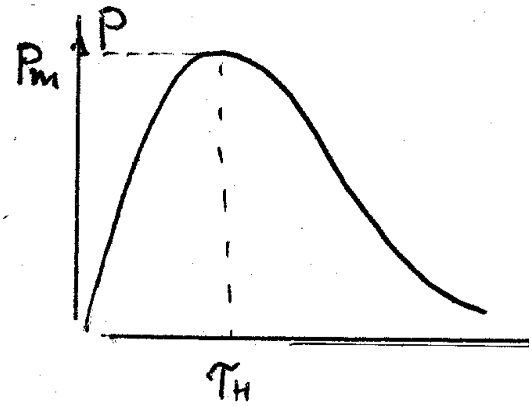

Figure 1:

complex than RT instability for perfect fluids and gases. This is added by uncertain strength properties of materials under high pressures $P > 20$ GPa.

Therefore, numerical simulation does not necessarily yield satisfactory results. However, sometimes simple analytical models can prove useful for qualitative estimates [1].

We have made ultimate velocity estimates for liners of various materials, using a simple phenomenological mode.

2 Numerical Model

Assume there is a pressure pulse generated at the interface of a plane solid layer, which drives this liner to acceleration. Sufficiently high-rate loading may result in strong shock waves and in the layer heating and melting. However, there may be shock-free loading of the layer, its strength remaining unchanged. The shock-free loading case is expressed as

$$\frac{dP}{dt} \leq \frac{\rho C^3}{H\left(1 + \frac{\rho}{2C^2}\left(\frac{\partial^2 P}{\partial \rho^2}\right)_S\right)} \tag{1}$$

or

$$\tau_H \geq \frac{HP_m}{\rho C^3}\left(1 + \frac{\rho}{2C^2}\left(\frac{\partial^2 P}{\partial \rho^2}\right)_S\right)$$

where H is the layer thickness, and C is the sound velocity.

The loss of stability is even contributed by weak compression and rarefaction waves circulating through the layer in the acceleration and reverse directions. The acceleration stability becomes the highest when the pressure rise time is equal to the time for two

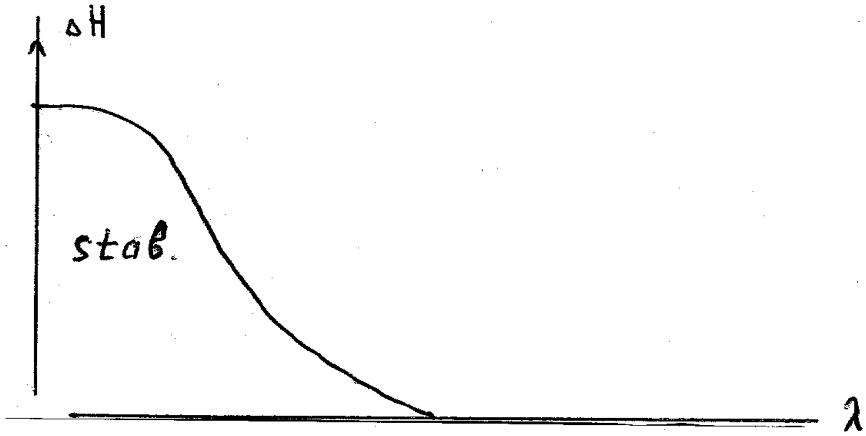

Figure 2:

or four sonic wave circulations through the layer

$$\tau_H \sim (2 \div 4)\frac{H}{C} \tag{2}$$

To avoid stalling, the characteristic pressure decay time should be also equal to or more than H/C

Depending on the initial conditions, there may be three behavior patterns for the layer being accelerated, including (a) disruption-free acceleration, (b) disruption during inertia flight following acceleration, and (c) disruption in acceleration.

Figure 2 shows typical stability and instability patterns in coordinates.

The following equation expresses the stability boundary of elasto-plastic incompressible layer

$$\frac{\Delta H}{H} = \frac{2\sigma_T}{P}\left(1 - \exp\left(-\frac{2\pi H}{\sqrt{3}\lambda_C}\right)\right)\left(\left(1 - \exp\left(-\frac{2\pi H}{\sqrt{3}\lambda_c}\right)\right)^2 - \left(\frac{\lambda_C P}{4\pi C_t^2 \rho H}\right)^2\right). \tag{3}$$

Here, σ_T is the yield point, P is the interface pressure, H is the layer thickness, C_t is the shear wave velocity in the layer, and ρ is the density.

Eq. (3) agrees rather well with numerical calculations and experimental data for loading pressures not very high. For higher pressures, i.e. $P > 20$ GPa, Eq. (3) overestimates the boundary value of H while yielding the correct critical wavelength value λ_c.

The layer non-uniformity in density as well as that in thickness may contribute to the perturbations growth. What can be shown is that a small difference in density is the same as the relative different in thickness $\frac{\Delta H}{H}$, e.g. Eq. (3) is also valid for the difference in density with $\frac{\Delta H}{H}$ substituted for $\frac{\Delta \rho}{\rho}$.

The perturbations with the wavelength about twice the critical value (as determined by Eq. (3)) grow most rapidly.

$$\lambda_m = 2\lambda_c. \tag{4}$$

For specified thickness difference H, the accelerating layer "lifetime" is determined by growth of perturbations with wavelength. Consider that perturbations with wavelength grow without resistance, i.e. similarly to the perfect fluid case. The growth of small perturbations in a thin perfect fluid layer ($\Delta H > H$) with initial sinusoidal thickness non-uniformity can be described by the following equations

$$X(t,x) = \frac{\Delta H}{H}\frac{\lambda_m}{8\pi}\exp\left(\sqrt{\frac{2\pi g}{\lambda_m}}t\right)\cos\left(\frac{2\pi x}{\lambda_m}\right) \tag{5}$$

$$Y(t,x) = \frac{\Delta H}{H}\frac{\lambda_m}{8\pi}\exp\left(\sqrt{\frac{2\pi g}{\lambda_m}}t\right)\sin\left(\frac{2\pi x}{\lambda_m}\right) \tag{6}$$

where $X(t,x)$ and $Y(t,x)$ are the substance displacements in the acceleration and normal directions.

For impulse loading, the mean values of acceleration should be used for Equations (3) and (4).

As it can be assumed, the layer disruption will occur when the strain value in the x direction is close to unity, i.e.

$$\varepsilon_x = \left(\frac{\partial X}{\partial x}\right)_m = \frac{\Delta H}{H}\exp\left(\sqrt{\frac{2\pi \bar{g}}{\lambda_m}}t\right) = 1 \tag{7}$$

This results in the following equation for the maximum achievable velocity:

$$u_m = \sqrt{\frac{\bar{g}\lambda_m}{2\pi}}\ln\left(\frac{4H}{\Delta H}\right) \tag{8}$$

The layer velocity may reach this value u_m; however, its disruption may occur some time later, due to inertia of the perturbation growth.

It is of interest to estimate the ultimate velocity for which there would be no layer disruption at the inertia stage of motion. To this effect, assume that no disruption will occur when perturbation kinetic energy is smaller than the work required to deform the layer to the plastic strain limit, i.e.

$$W \le \left(\frac{\sigma_T^2}{2E} + \sigma_T\delta_m\right)V \tag{9}$$

	ρ^2/cm^3	$C_t\text{cm/c}$	V	E(GPa)	δ_m	σ_T(GPa)
Fe	7.85	2.8	0.3	60	0.1-0.3	3
Ti	4.5	3.3	0.3	48	0.1-0.2	2
Br	1.86	8	0.1	130	0.02-0.05	1.5

Table 1: Characteristics of metals considered by the calculations.

where E is Young's modulus, V is the volume, $\frac{\sigma_T^2}{2E}$ is the elastic work of strain, and $\sigma_T\delta_m$ is the plastic work of strain.

The average kinetic energy of perturbation after unloading is

$$W \simeq \frac{\rho V}{2}\left(\left(\frac{\partial X}{\partial t}\right)^2 + \left(\frac{\partial Y}{\partial t}\right)^2\right) = \frac{\rho V \lambda_m \bar{g}}{64\pi}\exp\left(2\sqrt{\frac{2\pi g}{\lambda_m}}t\right) \tag{10}$$

By substituting (10) into (9), we find the maximum velocity for which no layer disruption will occur:

$$u_f \simeq \sqrt{\frac{\bar{g}\lambda_m}{8\pi}}\ln\left(\left(\frac{H}{\Delta H}\right)^2 \frac{64\pi\left(\frac{\sigma_T^2}{2E}+\sigma_T\delta_m\right)}{\rho\bar{g}\lambda_m}\right). \tag{11}$$

3 Estimating Ultimate Velocities for Liner Acceleration

The estimates have been done for typical mass thickness of liners which are used in laboratory accelerating devices, $(\rho H) = 0.2\text{g/cm}$. The materials considered were typical structural materials, such as steel, titanium, and also beryllium, which has a very high sound velocity. The peak layer loading pressure taken was 20 and 50 GPa. Table 1 gives the characteristics of the materials considered by the calculations.

The density difference of metals made by integrated techniques does not exceed the value $\frac{\Delta\rho}{\rho} = 10^{-4}$. The layer may have thickness difference brought to $\frac{\Delta H}{H} = 10^{-3}$. This is the value used by the calculations. Tables 2 and 3 summarize the data calculated by Eqs. (8) and (11).

Beryllium is considerably superior to Fe and Ti in maximum achievable velocity. This is due to its high stiffness-to-weight ratio characterized by shear wave velocity C_t.

As the pressure increases, there is a noticeable increase in the maximum achievable velocity. It should be noted, however, that higher pressure and accordingly shorter loading time may break the inequalities (1) and (2) which provide for low intensity compression and rarefaction waves resulting in the layer losing acceleration stability, heating and even melting.

	λ_c(cm)	λ_m(cm)	u_m (km/c)	u_f (km/c)
Fe	0.26	0.52	17	13
Ti	0.4	0.8	21	15
Be	1.5	3	40	24

Table 2: $P_m = 20$GPa.

	λ_c(cm)	λ_m(cm)	u_m (km/c)	u_f (km/c)
Fe	0.16	0.32	21	15
Ti	0.24	0.48	25	18
Be	0.9	1.8	49	28

Table 3: $P_m = 50$GPa.

Comparing the inequality (2) and the following relation between the velocity and the loading pulse parameters

$$u_m \sim \frac{P_m \tau_H}{\rho H}$$

yields the qualitative relationship for maximum pressure allowable for the layer acceleration

$$\rho_m < \frac{\rho C u_m}{4} \tag{12}$$

As suggested by (12), maximum loading pressures for steel, titanium and beryllium is between 100 and 200 GPa.

References

[1] Nizovtsev, P. N., Rayevsky, V. A., Approximate analytical solution of Rayleigh-Taylor instability problem in strong media, VANT. Ser. Teor. i Prikl. Fizika, 1991, No.3, p.11–17.